
Article:
Zhang, Y., Griffin, J., Scarratt, N.W. et al. (2 more authors) (2016) High efficiency arrays of polymer solar cells fabricated by spray-coating in air. Progress in Photovoltaics: Research and Applications, 24 (3). pp. 275-282. ISSN 1062-7995

https://doi.org/10.1002/pip.2665

High efficiency arrays of polymer solar cells fabricated by spray-coating in air

Yiwei Zhang[1], Jonathan Griffin[1], Nicholas W. Scarratt[1], Tao Wang[2, 1]*, David G. Lidzey[1]*

[1]Department of Physics and Astronomy, University of Sheffield, Sheffield, S3 7RH, UK

[2]School of Materials Science and Engineering, Wuhan University of Technology,

Wuhan, 430070, China

*E-mail: twang@whut.edu.cn,d.g.lidzey@sheffield.ac.uk

Abstract: We present bulk heterojunction organic solar cells fabricated by spray-casting both the PEDOT:PSS hole-transport layer (HTL) and active PBDTTT-EFT:$PC_{71}BM$ layers in air. Devices were fabricated in a (6 x 6) array across a large-area substrate (25 cm^2) with each pixel having an active area of 6.45mm^2. We show that the film uniformity and operational homogeneity of the devices are excellent. The champion device with spray cast active layer on spin cast PEDOT:PSS had an power conversion efficiency (PCE) of 8.75%, and the best device with spray cast active layer and PEDOT:PSS had a PCE of 8.06%. The impacts of air and light exposure of the active layer on device performance are investigated and found to be detrimental.

Keywords: Bulk heterojunction solar cells, PBDTTT-EFT:$PC_{71}BM$, Spray casting, Multi-pixel device

The increasing demands for energy have driven the development of new technologies. Photovoltaic devices (PVs) are in principle able to produce 'green' energy from sunlight. The photovoltaic effect has been observed since 1950s.[1] Since the first report in 1986 of a donor-acceptor organic photovoltaic (OPV) device[2], their performance has improved greatly as a result of significant research effort. Indeed, compared with conventional silicon based solar cells, OPVs combine the potential advantages of large-area production by low-cost solution processing techniques on mechanically flexible substrates.[3-5] The energy payback time (EPBT) of OPVs is also believed to be competitive compared to other types of PV technologies because lower-energy mass-production process (e.g. roll-to-roll processing), can be used to fabricate OPVs and because the thermal budget for OPV fabrication is also lower.[6] The power conversion efficiencies (PCEs) of such devices have increased steadily, with values of over 10% being reported recently for both single-junction and multi-junction bulk hetrojunction devices (BHJ); a result considered a significant milestone in the development of OPVs.[7, 8]

The design and synthesis of new conjugated polymers has been one of the main drivers in the improvement of OPV efficiency, with polymers based on benzodithiophene (BDT) attracting significant research interest.[9-14] Recently, a new polymer,poly[4,8-bis(5-(2-ethylhexyl)thiophen-2-yl)-benzo[1,2-b;4,5-b']dithiophene-2,6-diyl-alt-(4-(2-ethylhexyl)-3-fluorothieno[3,4-b]thiophene-)-2-carboxylate-2-6-diyl)] (PBDTTT-EFT) has been used to create OPVs having PCEs in excess of 9%[15, 16]. Notably, such PBDTTT-EFT based devices have been fabricated using spin-coating in a nitrogen-filled glove box. Spin-coating is a wasteful-technique, as much valuable material is 'lost' during the coating process. It is also not compatible with deposition onto a moving web, making it an unsuitable process for large-area device manufacture. In contrast, spray-coating is technique compatible with high-volume manufacture process that has been used to fabricate OPVs having efficiency similar to those created by spin casting.[17-19] For example, OPVs based on a blend of poly(3-hexylthiophene-2,5-diyl) (P3HT) and phenyl-C61-butyric acid methyl ester ($PC_{61}BM$) were fabricated using an airbrush spray coating technique and had a PCE of 4.1%; a value typical of spin-cast OPVs based on this photoactive layer. [20] Spray-coating has also been used to fabricate OPV devices using a series of different carbazole/benzothiadiazole based polymer-fullerene blends, with spin- and spray-coated devices having comparable efficiency. [19]

Such progress has motivated us to explore the extent to which we can scale-up the spray-coating of OPV devices; a necessary step in the pathway by which any technology makes a

transition from laboratory to factory. To explore the uniformity of devices as their active area of the device is increased, we have fabricated PBDTTT-EFT/$PC_{71}BM$ based OPV devices by spray-coating in air onto glass substrates having an area of (5 x 5) cm^2. Here, each substrate was sub-divided into an array of 36 pixels, with each pixel having an active area of 2.54 x 2.54 mm^2. We have tested the efficiency of the pixels within such arrays and find that when the active layer was spray-coated, a maximum pixel PCE of 8.75% is obtained, with the average PCE of all 36 pixels being 7.86%. Devices in which both the poly(3,4-ethylenedioxythiophene)-polystyrene sulfonate (PEDOT:PSS) hole transport layer (HTL) and the PBDTTT-EFT/$PC_{71}BM$ photoactive layer are spray-coated had a maximum pixel PCE of 8.06% with the average pixel PCE being 7.50%. To the best of our knowledge, these are the highest efficiency OPV device fabricated by spray casting both photoactive and HTL layers.

The molecular structures of electron-donor polymer PBDTTT-EFT and electron-acceptor fullerene$PC_{71}BM$ are shown in Figure 1a. The PBDTTT-EFT was purchased from Solarmer Energy (Beijing) Inc. and had an M_w of 114,054 g/mol and a PDI of 3.01. PBDTTT-EFT has an optical band-gap of 1.58 eV, highest occupied molecular orbital (HOMO) level and lowest unoccupied molecular orbital (LUMO) level at -5.24 and -3.66eV respectively. This relatively low band-gap, together with efficient charge extraction, contributes to the high PCE of PBDTTT-EFT OPVs.

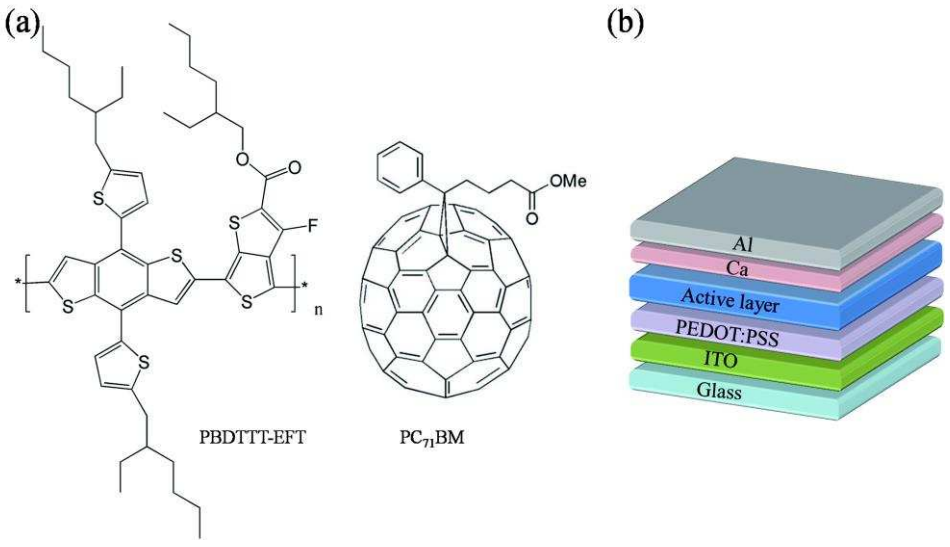

Fig. 1(a) The molecular structure of PBDTTT-EFT and $PC_{71}BM$. (b) A schematic of the device structure explored.

Devices were fabricated using a Prism 300 ultra-sonic spray-coater, supplied by Ultrasonic Systems Inc. The devices fabricated were based on the structure Glass/ITO/PEDOT:PSS/PBDTTT-EFT:$PC_{71}BM$/Ca/Al, as shown schematically in Figure 1b. For comparative purposes, the PEDOT:PSSHTL was prepared by both spin- and spray coating. To spin-cast PEDOT:PSS (Clevios™ AI 4083), it was dispensed onto the ITO-coated substrate which was rotating at 5000 rpm for 30s to form a film having a thickness of approximately 30 nm. To spray-coat PEDOT:PSS, it was necessary to mix the Clevios™ AI 4083 solution with 2-Propanol (IPA) and ethylene glycol (EG) at a volume ratio of 1:8:1. Here the IPA improved the initial wetting on the underlying ITO substrate, with the EG increasing film viscosity and also suppressing de-wetting as IPA evaporated from the film. We also found that it was necessary to hold the substrate at 50°C during the spray-coating process to encourage surface wetting by reducing the viscosity of the ink and optimizing the drying time of the film. Using such techniques, we were able to spray-cast a uniform PEDOT:PSS film having a thickness of ~ 30 nm. We have used atomic force microscopy (AFM) to explore the surface morphology of PEDOT:PSS films prepared by spin and spray casting on ITO as shown in Figure 2a and b. We determine a root mean square (RMS) roughness of the spin cast PEDOT:PSS film over 5x5 μm^2 to be 1.4nm. Although the spray cast counterpart was slightly rougher (having a RMS roughness of 2.9 nm), this did not prove detrimental to its performance as a HTL layer.

To prepare the active layer, PBDTTT-EFT and $PC_{71}BM$ were mixed at a ratio of 1:1.5 by weight, and dissolved (at a final concentration of 5 mg/ml) in a chlorobenzene (CB) solvent. To this was added 3% (by volume) of 1,8-diiodooctane (DIO), as this has been found to dramatically improve the efficiency of polymer:fullerene OPV devices.[21] The high boiling point CB solvent (ca. 130°C) was chosen to minimize evaporation during the spray-coating process. The spray-head substrate distance and lateral coating-speed were determined by careful optimization such that a uniform and continuous wet film could be deposited on the device substrate. We have previously described the effect of such coating parameters, [19] and give further details in Experimental Methods. This optimisation was found crucial to avoid the formation of unconnected “domains” within the active layer which otherwise form if the spray droplets are not able to merge and coalesce after deposition on the substrate. Again, the substrate was held at 50°C during spray-coating to suppress de-wetting of the solution during drying.[19] In all cases, spray coating was performed in air, with devices being transferred immediately after coating to a nitrogen filled glove-box. By adjusting the

spray-coating parameters, we were also able to control the thicknesses of the active layer. Through a series of optimization measurements we determined an optimum thickness for device efficiency as 100nm; a value similar to that identified in equivalent spin-cast devices.[16]

It is known that the morphology of the active layer have great influence on the device performance.[22] We have measured the surface morphology of spray cast PBDTTT-EFT:$PC_{71}BM$ blend films prepared on spin and spray cast PEDOT:PSS substrates using AFM, as shown in Figures 2d and e. As a reference, we also show the morphology of a spin cast PBDTTT-EFT:$PC_{71}BM$ blend film prepared on a spin cast PEDOT:PSS film (see Figure 2c). It can be seen that all the PBDTTT-EFT:$PC_{71}BM$ films are characterized by high surface uniformity, with the RMS roughness of the spray-coated active layer being as low as 0.5nm; a value less than its spin cast counterpart (which had a RMS roughness of 1.6 nm). We speculate that the reduced roughness of the spray-coated layers result from the low concentration and reduced viscosity of the ink. Such reduced viscosity results in the rapid coalescence of individual spray droplets into a continuous film. Note that we did not observe any large-scale $PC_{71}BM$ aggregates or phase-separated domains at the film surface. It has been shown that the surface of a PBDTTT-EFT:$PC_{71}BM$ blend film is slightly enriched by the polymer component (containing around 60% of PBDTTT-EFT), and that $PC_{71}BM$ aggregation is suppressed due to the presence of DIO during solution casting. [15] For this reason we conclude that the surface structure observed here is unlikely to originate from coarse-scale phase-separation between the polymer and the fullerene.

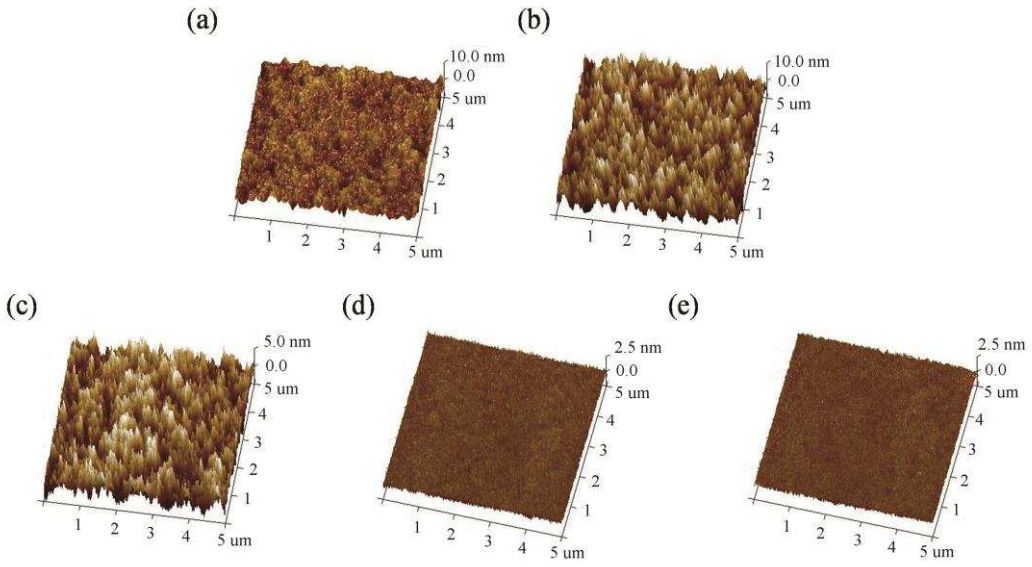

Fig. 2 AFM surface topography of (a) spin cast PEDOT:PSS, (b) spray cast PEDOT:PSS, (c) spin cast PBDTTT-EFT:$PC_{71}BM$ on spin cast PEDOT:PSS. Part (d) shows the topography of a spray cast PBDTTT-EFT:$PC_{71}BM$ on spin cast PEDOT:PSS and (e) spray cast PBDTTT-EFT:$PC_{71}BM$ on spray cast PEDOT:PSS.

The spray-cast and spin-cast films were fabricated into OPV devices using the techniques described in Experimental Methods. An array of typical devices is shown in figure 3a. Here, 6 ITO (anode) and 6 Ca / Al (cathode) strips (both having a width of 2.54 mm) are deposited in orthogonal directions, creating 36 individual OPV pixels. We note that recent work has demonstrated the entire fabrication of OPVs (including electrodes and active layers) using solution processing-techniques. [23-25] Indeed, it was shown that devices could be created using solution processed silver nanowires or grids as the device cathode or anode; a result that could potentially be used to eliminate vacuum-dependent techniques from a device manufacture process. In this work however, we have utilized a composite Ca/Al cathode deposited by thermal evaporation and instead focus on the realisation of high performance OPVs having both their hole transport layer and active layer deposited by spray coating in air. We envisage that the development of high performance OPVs using all-solution processes could be realized by integrating our techniques with other solution-processed cathode technologies as reported in the literature.

For testing, each OPV pixel was illuminated individually through a 3.14 mm^2 aperture mask to define the exposed area, whilst ensuring that the remaining 35 pixels were not exposed. The results of a typical experiment on a device that incorporated a spin cast PEDOT:PSS layer and a spray cast active layer are summarized in Table S1, with a 3D map of device PCE plotted in Figure 3b. It can be seen that all pixels within the array are operational, and that a PCE of 8.75% is determined for one of the pixels. Using a simple statistical analysis, we find that the pixels have an average PCE of 7.86% with the standard deviation of0.60.A histogram of device efficiency is plotted in Figure 3d, which shows that around 25% pixels from the array have a PCE between 7.96 and 8.16%. Figure 3c plots the efficiency across an array of devices in which both the HTL and active layer were deposited by spray-coating. Device efficiency is also tabulated in Table S2. Again, every single pixel is functional, with the peak PCE being 8.06%, the average PCE being 7.50% with a standard deviation of 0.30. Interestingly, it can be seen that the efficiency of the spray-cast devices are not significantly reduced at the device edges as is observed in the spin-cast device. We believe this originates from a greater degree of uniformity at the edges of the spray-cast films. A histogram of device efficiencies is plotted

in Figure 3e, from which we determine that 28% of pixels have a PCE between 7.6 and 7.8%, with 78% of pixels having a PCE between 7.2 and 7.8%. The relatively narrow distribution in device efficiency is also consistent with a promising degree of uniformity of the spray cast layers.

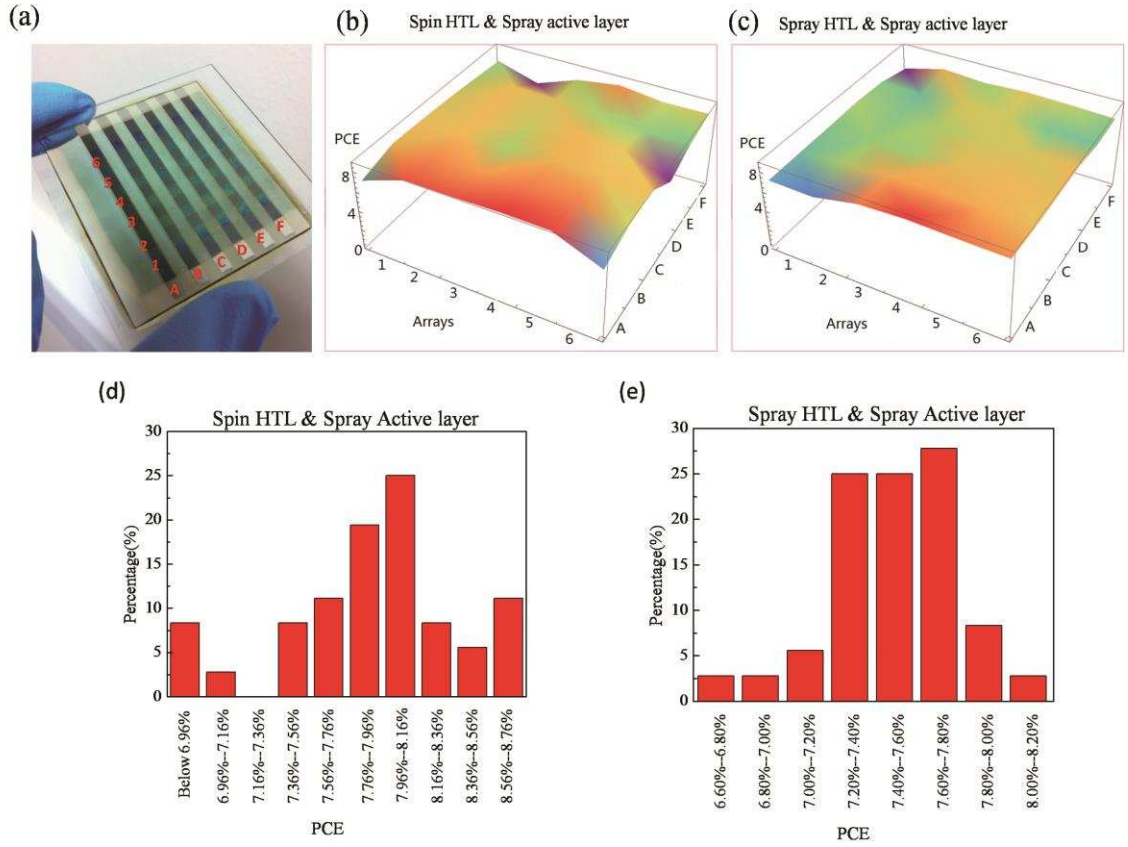

Fig. 3 (a) Image of a large-area, arrays of OPV device. In part (b) and (c), the PCE of every single pixel of devices fabricated by different casting technique as indicated accordingly is presented. Distribution of PCEs from 36 array devices made of (d) spin HTL and spray active layer and (e) spray HTL and spray active layer.

In Figure 4 we plot the J-V curve of the device from each of the arrays presented in Figure having the highest PCE. For completeness we also plot the J-V curve of a device in which both the HTL and the active layer were deposited by spin casting in air and nitrogen-filled glove box, respectively. For each type of device, we record key metrics in Table 1. It can be seen that devices in which both HTL and active layers were deposited by spin-coating in the glove-box had a maximum PCE of 9.35%; a value consistent with other comparable devices reported in the literature. [15, 16] By recording dark J-V measurements (Figure S1), we determine the electron and hole mobility from control devices in which transport is either

dominated by electrons or holes. From such measurements we determine $\mu_{electron}$ and μ_{hole} as $(3.8\pm0.1)x10^{-4}$ $cm^2V^{-1}s^{-1}$ and $(2.0\pm0.1)x10^{-4}$ cm^2 V^{-1} s^{-1} respectively.

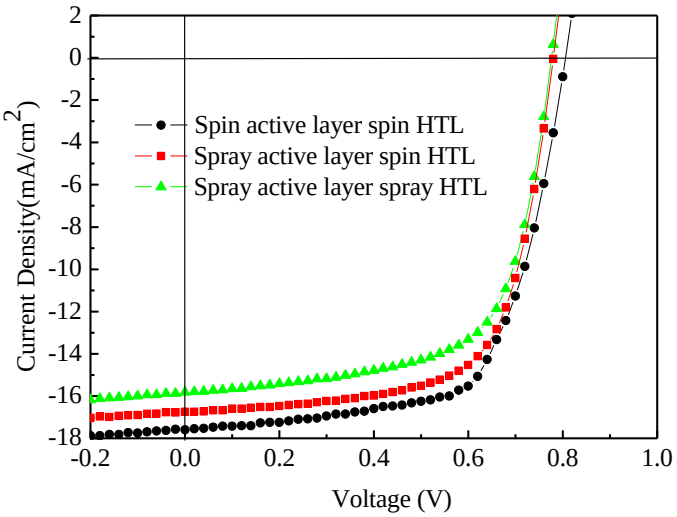

Fig. 4 J-V curves of OPV devices incorporating layers by different film casting methods.

Table 1. Device metrics of peak and average PBDTTT-EFT/$PC_{71}BM$ OPVs fabricated by spin and spray casting on spin and spray cast PEDOT:PSS.

Device type	J_{SC}(mA/cm^2)	V_{OC}(V)	FF(%)	PCE(%)
Spin active layer &spin HTL*	17.60 (17.06±0.21)	0.81 (0.80±0.01)	65.61 (65.01±0.53)	9.35 (9.11±0.15)
Spray active layer &spin HTL	16.75 (15.68±0.76)	0.78 (0.77±0.09)	66.97 (65.00±2.23)	8.75 (7.86±0.60)
Spray active layer &spray HTL	15.83 (15.16±0.29)	0.78 (0.77±0.04)	65.28 (64.29±2.09)	8.06 (7.50±0.30)

* The active layer was spin cast in a nitrogen-filled glove box.

It is apparent that the peak (average) PCE of devices with both HTL and active layer fabricated by spray casting is slightly reduced to 8.06% (7.50%) comparing to devices in which the HTL is deposited by spin casting. We attribute this reduction to the increased conductivity of spray cast PEDOT:PSS layer in which the organic solvent IPA and additive

ethylene glycol (EG) were used to assist the film formation process. Our measurements indicate that the electrical conductivity of the spray cast PEDOT:PSS film is 4.45 S cm^{-1}; a value significantly larger than that of the spin cast PEDOT:PSS films that is around 0.002 S cm^{-1}. It is well known that organic solvents and process additive scan change both the degree of phase-separation between PEDOT and PSS within a PEDOT:PSS film, and increase the molecular orientation of the PEDOT component, leading to an increase in electrical conductivity of several orders of magnitude.[26, 27] For a single pixel, high conductivity is beneficial for the extraction of charge carriers. [28, 29] However, in the pixelated device arrays explored here, the high lateral conductivity of PEDOT:PSS layer is likely to result in significant current-spreading, with lateral charge transport resulting in charges travelling outside the region defined by the aperture mask through which each individual device is illuminated. We believe this current spreading within the large array of devices explored here contributes to the lower device efficiencies recorded in devices that incorporate a high-conductivity spray-cast PEDOT:PSS layer (see Table 1). In our unpublished work, we have explored the effect of pixel size on OPV efficiency using a spray-cast PCDTBT:$PC_{70}BM$ blend. Here, we found that device efficiency was reduced by around 17% when the active area of the device was increased from 4 mm^2 to 165 mm^2 due to the increased serial resistance of the ITO anode. It is expected that scale-up of the device reported here will also be reduced as active area is increased.

Returning to Table 1 and Figure 4, it can be seen that the maximum PCE of devices in which both HTL and active layers were spin-coated is larger than those of devices in which spray-coating was used to deposit either the active layer or both the active and HTL layers. Here, the device efficiency of the spray-coated devices is reduced by the slightly lower values of J_{SC} and V_{OC} although the fill-factors (FFs) of all types of device are similar at around 65%. We speculate therefore that the slightly reduced performance of devices that incorporate a spray cast active layer may originate from a number of factors, including exposure to oxygen, moisture and light.[30-33]

To confirm our speculation, we made devices in which a spin cast active layer fabricated in a nitrogen-glove box was exposed to air under normal room-light conditions (white light having an estimated optical intensity of 5 W/m^2) for varying amounts of time. A second series of experiments exposed samples to air in the dark. After air-exposure, the substrates were then transferred back to the glove box and a cathode was evaporated onto the film surface to create a series of devices. The normalized PCE of devices having different air-exposure times (both

in the light and the dark) is shown in Figure 5. It can be seen that exposing the active layer to air decreases device efficiency, however this effect is significantly more pronounced when this exposure occurs in the light. In particular, a 30 minute air exposure in the dark resulted in a device having a PCE that was 81% of its unexposed control. However a similar exposure in the light results in a device having a PCE that was 7% of its initial value. We note that work on a related BDT based polymer (PTB7) has concluded that degradation of the polymer results from a photochemical reaction that required the presence of both oxygen and light.[34, 35]

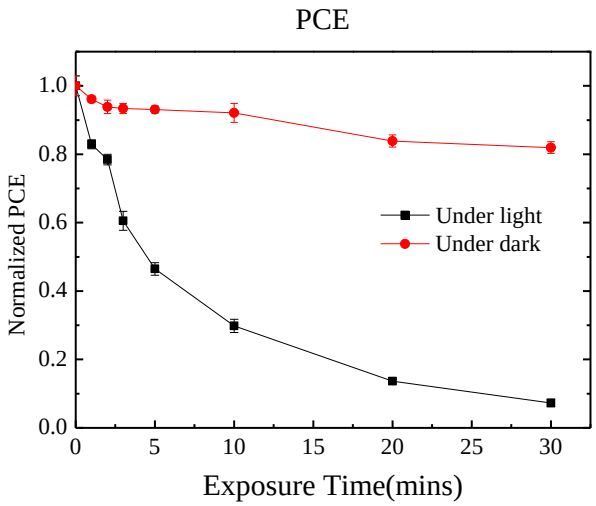

Figure 5. Normalized PCE of devices with different exposure time.

We have previously fabricated OPVs by spray coating in air, with the active semiconductor layer based on a series of different polycarbazole copolymers. Importantly, such measurements did not show any evidence of reduction in device performance as a result of air exposure – even for extended periods.[19] The work presented here clearly demonstrates however that PBDTTT-EFT based OPV devices undergo a degradation in performance on exposure to air, although this process can be partially suppressed by minimising the exposure of the active semiconductor material to light. Our results indicate therefore that any practical air-based manufacture process based on this material system would require careful control of ambient lighting conditions.

Conclusion

We have fabricated large-area, pixelated PBDTTT-EFT:$PC_{71}BM$ organic solar cells by spray casting the PEDOT:PSS and/or the photoactive layers under ambient conditions. By

optimizing the fabrication process, we fabricated OPV devices having a spray-cast active layer (but spin-cast HTL layer) with PCEs of up to 8.75%; a value that is comparable with devices fabricated by spin-casting alone. For devices having both spray-cast active layer and HTL a maximum device PCE of 8.06% was obtained. Control measurement demonstrated that some reduction in device efficiency of devices that are spray-cast in air results from oxidation of the PBDTTT-EFT polymer, and that optimum device efficiency occurs when the exposure of the active semiconductor to light and air is minimised. Our results further confirm that spray coating is a promising technique that is capable of fabricating high efficiency organic photovoltaic devices over large-area substrates.

Acknowledgements

We thank financial support from EPSRC via grant EP/I028641/1 "Polymer/fullerene photovoltaic devices: new materials and innovative processes for high-volume manufacture" and EP/M014797/1 "SUPERGEN Supersolar Solar Energy Hub". Y.Z. thanks the University of Sheffield for the provision of a PhD scholarship. T.W. acknowledges funding support from the Recruitment Program of Global Experts (1000 Talents Plan) of China

Experimental section

Glass substrates (5 cm x 5 cm) coated with pre-patterned ITO were purchased from Ossila Limited. The substrates were sequentially cleaned by sonication in 10% (wt%) sodium hydroxide solution, Hellmanex solution, IPA and deionised water. Substrates were then dried using a jet of compressed nitrogen and then baked at 120°C for 5 minutes before use. PEDOT:PSS (HC Stark Clevios P VP AI4083) was filtered through a 0.45 μm PVDF filter before spin coating at 5000 rpm to form a 30nm thick hole-transport layer (HTL). The HTL was then thermally annealed at 120°C for 20 minutes before use. To spray-cast the PEDOT:PSS solution it was first filtered and then mixed with IPA and ethylene glycol at a volume ratio of 1:8:1. It was then spray cast onto the cleaned substrates forming a uniform film ca. 30 nm thick.

The ultra-sonicspray-coater system used in this work (a Prism 300) was supplied by Ultrasonic Systems Inc., andutilizedan ultra-sonic (35 kHz) vibrating tip. In this type of coater, the ink of interest is directed to the tip with the tip vibration sgenerating an aerosol that is then directed to a surface of inte restusing a nitrogen gas jet. This nozzleless spray technique minimizes droplet coalescence before reaching the substrate and permit the creation of highly-

uniform thin-films overrelatively large areas. By varying the height of the tip above the substrate as well as the lateral velocityof the tip and the nitrogen gas pressure during spray deposition, it is possible to control film uniformity and thickness. To deposit a PEDOT:PSS film, it was determined that a tip-surface separation, lateral tip velocity and nitrogen gas pressure of 70 mm, 80 mm/s and 10 psi respectively could be used to create a uniform PEDOT:PSS film having a thickness of 30 nm. During the spray coating,the substrate was held at 50 ºC to aid film wetting. In all cases, the lab humidity during spray-coating was typically 35 - 40% R.H.

The PBDTTT-EFT was purchased from Solarmer Energy (Beijing) Inc. $PC_{71}BM$ was purchased from Ossila Ltd. All materials were used as received. PBDTTT-EFT and $PC_{71}BM$ were blended together at a ratio of 1:1.5 (w/w) and dissolved into cholorobenzene with 3% (vol%) DIO as solvent additive at a concentration of 5 mg/ml. The PBDTTT-EFT:$PC_{71}BM$ ink was spray cast on PEDOT:PSS films prepared by either spin or spray casting. For the deposition of active layer, the substrate temperature was held at 50ºC, with the tip-surface separation, lateral coating velocity and nitrogen gas-pressure being 45 mm, 55 mm/s and 10 psi respectively. This technique permitted films to be deposited having a thickness of 100 nm. Control over active-layer thickness is important to optimise device efficiency; specifically, thinner films led to a reduced Jsc, while films that were too thick had reduced fill factor. After the spray cast active layer was virtually dry, the devices were immediately transferred into a nitrogen glove box. A cathode consisting of 5nm Ca and 100nm Al was thermally evaporated onto the active layer through a shadow mask to form the cathode. Finally, devices were encapsulated using a glass slide and UV-curable epoxy glue. As a control, reference spin cast devices were prepared from a 30 mg/ml solution of PBDTTT-EFT/$PC_{71}BM$ (1:1.5 (w/w)) in a chlorobenzene solution, having an active-layer thickness of around 100 nm. The reference devices were prepared on (2x1.5) cm^2 substrates that each contained 6 pixels having individual active areas of 6.4 mm^2. To study the mobility of the materials used, we have fabricated devices in which charge transport is dominated by one type of charge carrier; hole-dominated devices consisted of a structure based on Glass/ITO/PEDOT:PSS/active layer/Au, while those of the electron-dominated devices were based on Glass/ITO/Al/active layer/Ca/Al. All J-V testing was conducted using a Newport 92251A-1000 AM 1.5 solar simulator, which had been calibrated by a NREL standard silicon solar cell to assure a power output of 100 mW cm^{-2}. An aperture mask was placed over the devices to accurately define a test area of 3.14 mm^2 on each pixel and to eliminate the influence of stray and wave guided light.

AFM measurements were acquired using a Veeco Dimension 3100 operating in tapping mode.

References

1 G. A. Chamberlain, Organic solar cells: A review. Solar Cells 1983; **8**: 47-83.

2 C. W. Tang, 2-Layer Organic Photovoltaic Cell. Applied Physics Letters 1986; **48**: 183-185.

3 M. Scharber, N. Sariciftci, Efficiency of Bulk-Heterojunction Organic Solar Cells. Progress in Polymer Science 2013; **38**: 1929-1940.

4 J. J. M. Halls, C. A. Walsh, N. C. Greenham, E. A. Marseglia, R. H. Friend, S. C. Moratti, A. B. Holmes, Efficient Photodiodes from Interpenetrating Polymer Networks. Nature 1995; **376**: 498-500.

5 G. Yu, J. Gao, J. C. Hummelen, F. Wudl, A. J. Heeger, Polymer Photovoltaic Cells - Enhanced Efficiencies Via a Network of Internal Donor-Acceptor Heterojunctions. Science 1995; **270**: 1789-1791.

6 S. B. Darling, F. You, The case for organic photovoltaics. RSC Advances 2013; **3**: 17633-17648.

7 J. D. Chen, C. Cui, Y. Q. Li, L. Zhou, Q. D. Ou, C. Li, Y. Li, J. X. Tang, Single-Junction Polymer Solar Cells Exceeding 10% Power Conversion Efficiency. Advanced Materials 2014; **27**: 1035-1041.

8 M. A. Green, K. Emery, Y. Hishikawa, W. Warta, E. D. Dunlop, Solar cell efficiency tables (Version 45). Progress in Photovoltaics: Research and Applications 2015; **23**: 1-9.

9 H.-Y. Chen, J. Hou, S. Zhang, Y. Liang, G. Yang, Y. Yang, L. Yu, Y. Wu, G. Li, Polymer solar cells with enhanced open-circuit voltage and efficiency. Nature Photonics 2009; **3**: 649-653.

10 Y. Y. Liang, L. P. Yu, A New Class of Semiconducting Polymers for Bulk Heterojunction Solar Cells with Exceptionally High Performance. Accounts of Chemical Research 2010; **43**: 1227-1236.

11 L. Huo, J. Hou, Benzo[1,2-b:4,5-b[prime or minute]]dithiophene-based conjugated polymers: band gap and energy level control and their application in polymer solar cells. Polymer Chemistry 2011; **2**: 2453-2461.

12 H. Zhou, L. Yang, A. C. Stuart, S. C. Price, S. Liu, W. You, Development of Fluorinated Benzothiadiazole as a Structural Unit for a Polymer Solar Cell of 7 % Efficiency. Angewandte Chemie International Edition 2011; **50**: 2995-2998.

13 C. Cui, W.-Y. Wong, Y. Li, Improvement of open-circuit voltage and photovoltaic properties of 2D-conjugated polymers by alkylthio substitution. Energy & Environmental Science 2014; **7**: 2276-2284.

14 L. Ye, S. Zhang, L. Huo, M. Zhang, J. Hou, Molecular Design toward Highly Efficient Photovoltaic Polymers Based on Two-Dimensional Conjugated Benzodithiophene. Accounts of Chemical Research 2014; **47**: 1595-1603.

15 W. Huang, E. Gann, L. Thomsen, C. Dong, Y.-B. Cheng, C. R. McNeill, Unraveling the Morphology of High Efficiency Polymer Solar Cells Based on the Donor Polymer PBDTTT-EFT. Advanced Energy Materials 2015; **5**: 1401259.

16 S. Zhang, L. Ye, W. Zhao, D. Liu, H. Yao, J. Hou, Side Chain Selection for Designing Highly Efficient Photovoltaic Polymers with 2D-Conjugated Structure. Macromolecules 2014; **47**: 4653-4659.

17 D. J. Vak, S. S. Kim, J. Jo, S. H. Oh, S. I. Na, J. W. Kim, D. Y. Kim, Fabrication of organic bulk heterojunction solar cells by a spray deposition method for low-cost power generation. Applied Physics Letters 2007; **91**: 081102.

18 C. Girotto, D. Moia, B. P. Rand, P. Heremans, High-Performance Organic Solar Cells with Spray-Coated Hole-Transport and Active Layers. Advanced Functional Materials 2011; **21**: 64-72.

19 T. Wang, N. W. Scarratt, H. A. Yi, A. D. F. Dunbar, A. J. Pearson, D. C. Watters, T. S. Glen, A. C. Brook, J. Kingsley, A. R. Buckley, M. W. A. Skoda, A. M. Donald, R. A. L. Jones, A. Iraqi, D. G. Lidzey, Fabricating High Performance, DonorAcceptor Copolymer Solar Cells by Spray-Coating in Air. Advanced Energy Materials 2013; **3**: 505-512.

20 G. Susanna, L. Salamandra, T. M. Brown, A. Di Carlo, F. Brunetti, A. Reale, Airbrush spray-coating of polymer bulk-heterojunction solar cells. Solar Energy Materials and Solar Cells 2011; **95**: 1775-1778.

21 H.-C. Liao, C.-C. Ho, C.-Y. Chang, M.-H. Jao, S. B. Darling, W.-F. Su, Additives for morphology control in high-efficiency organic solar cells. Materials Today 2013; **16**: 326-336.

22 W. Chen, M. P. Nikiforov, S. B. Darling, Morphology characterization in organic and hybrid solar cells. Energy & Environmental Science 2012; **5**: 8045-8074.

23 D. Angmo, S. A. Gevorgyan, T. T. Larsen-Olsen, R. R. Søndergaard, M. Hösel, M. Jørgensen, R. Gupta, G. U. Kulkarni, F. C. Krebs, Scalability and stability of very thin, roll-to-roll processed, large area, indium-tin-oxide free polymer solar cell modules. Organic Electronics 2013; **14**: 984-994.

24 F. Guo, X. Zhu, K. Forberich, J. Krantz, T. Stubhan, M. Salinas, M. Halik, S. Spallek, B. Butz, E. Spiecker, T. Ameri, N. Li, P. Kubis, D. M. Guldi, G. J. Matt, C. J. Brabec, ITO-Free and Fully Solution-Processed Semitransparent Organic Solar Cells with High Fill Factors. Advanced Energy Materials 2013; **3**: 1062-1067.

25 T. M. Eggenhuisen, Y. Galagan, A. F. K. V. Biezemans, T. M. W. L. Slaats, W. P. Voorthuijzen, S. Kommeren, S. Shanmugam, J. P. Teunissen, A. Hadipour, W. J. H. Verhees, S. C. Veenstra, M. J. J. Coenen, J. Gilot, R. Andriessen, W. A. Groen, High efficiency, fully inkjet printed organic solar cells with freedom of design. Journal of Materials Chemistry A 2015; **3**: 7255-7262.

26 D. Alemu Mengistie, P.-C. Wang, C.-W. Chu, Effect of molecular weight of additives on the conductivity of PEDOT:PSS and efficiency for ITO-free organic solar cells. Journal of Materials Chemistry A 2013; **1**: 9907-9915.

27 W. Zhang, B. Zhao, Z. He, X. Zhao, H. Wang, S. Yang, H. Wu, Y. Cao, High-efficiency ITO-free polymer solar cells using highly conductive PEDOT:PSS/surfactant bilayer transparent anodes. Energy & Environmental Science 2013; **6**: 1956-1964.

28 B. Zacher, N. R. Armstrong, Modeling the Effects of Molecular Length Scale Electrode Heterogeneity in Organic Solar Cells. The Journal of Physical Chemistry C 2011; **115**: 25496-25507.

29 Y. H. Kim, C. Sachse, M. L. Machala, C. May, L. Müller‐Meskamp, K. Leo, Highly conductive PEDOT: PSS electrode with optimized solvent and thermal post‐treatment for ITO‐free organic solar cells. Advanced Functional Materials 2011; **21**: 1076-1081.

30 M. Jorgensen, K. Norrman, S. A. Gevorgyan, T. Tromholt, B. Andreasen, F. C. Krebs, Stability of Polymer Solar Cells. Advanced Materials 2012; **24**: 580-612.

31 M. P. Nikiforov, J. Strzalka, S. B. Darling, Delineation of the effects of water and oxygen on the degradation of organic photovoltaic devices. Solar Energy Materials and Solar Cells 2013; **110**: 36-42.

32 Q. D. Yang, T.-W. Ng, M.-F. Lo, F. Y. Wang, N. B. Wong, C.-S. Lee, Effect of Water and Oxygen on the Electronic Structure of the Organic Photovoltaic. The Journal of Physical Chemistry C 2012; **116**: 10982-10985.

33 M. Jorgensen, K. Norrman, F. C. Krebs, Stability/degradation of polymer solar cells. Solar Energy Materials and Solar Cells 2008; **92**: 686-714.

34 Y. W. Soon, H. Cho, J. Low, H. Bronstein, I. McCulloch, J. R. Durrant, Correlating triplet yield, singlet oxygen generation and photochemical stability in polymer/fullerene blend films. Chemical Communications 2013; **49**: 1291-1293.

35 J. Razzell-Hollis, J. Wade, W. C. Tsoi, Y. Soon, J. Durrant, J. S. Kim, Photochemical stability of high efficiency PTB7:PC70BM solar cell blends. Journal of Materials Chemistry A 2014; **2**: 20189-20195.